Spectral Efficiency of Distributed Antenna Network Using MIMO Spatial Multiplexing

Shinya KUMAGAI† Ryusuke MATSUKAWA† Tatsunori OBARA†

Tetsuya YAMAMOTO† and Fumiyuki ADACHI‡

Dept. of Electrical and Communication Engineering, Graduate School of Engineering, Tohoku University
6-6-05, Aza-Aoba, Aramaki, Aoba-ku, Sendai, 980-8579, JAPAN
E-mail: †{kumagai, matsukawa, obara, yamamoto}@mobile.ecei.tohoku.ac.jp ‡adachi@ecei.tohoku.ac.jp

Abstract—**Multiple-input multiple-output (MIMO) spatial multiplexing is known to increase the transmission rate without bandwidth expansion. However, in cellular networks (CNs), the transmission rate of a user close to the cell edge significantly degrades because the received signal-to-interference plus noise power ratio (SINR) degrades due to the presence of strong co-channel interference (CCI) from neighboring cells. Distributed antenna network (DAN), in which many antennas are spatially distributed over the cell, is suitable for MIMO spatial multiplexing because the received SINR improves over the entire cell. In this paper, assuming block transmission with cyclic prefix (CP) insertion, we theoretically derive an expression for the downlink spectral efficiency of DAN-MIMO spatial multiplexing in a multi-cell environment. Then, we propose the optimal and suboptimal transmit power allocation schemes for DAN-MIMO spatial multiplexing. We evaluate the spectral efficiency distribution by Monte Carlo numerical computation method to show that DAN allows single frequency reuse and achieves higher spectral efficiency compared to CN.**

Keywords; Distributed antenna, MIMO spatial multiplexing, spectral efficicency, multi-cell environment, frequency-selective channel

I. INTRODUCTION

In the next generation mobile communication systems, broadband services are demanded. However, the available bandwidth is limited. Multiple-input multiple-output (MIMO) spatial multiplexing [1] is a powerful technique used to increase the transmission rate without bandwidth expansion.

The broadband wireless channel is characterized by path loss, shadowing loss, and frequency-selective fading [2]. In conventional cellular networks (CNs), multiple antennas for spatial multiplexing are co-located at each base station (BS). Therefore, the received signal power near the cell edge often drops. In addition, the same frequency is reused in spatially separated cells to efficiently utilize the limited frequency bandwidth. Therefore, the receiver suffers from co-channel interference (CCI) from neighboring cells [2]. As a result, the received signal-to-interference plus noise power ratio (SINR) near the cell edge significantly drops, and the transmission rate significantly degrades even if MIMO spatial multiplexing is used in CNs. The distance between two co-channel cells has to be increased to improve the received SINR. However, this reduces the bandwidth allocated to each cell for the given system bandwidth (lower spectral efficiency).

Distributed antenna network (DAN) [3]-[5] can improve the spectral efficiency by using MIMO spatial multiplexing. In DAN, a number of antennas are spatially distributed in each cell and connected by optical fiber cables to the signal processing center (SPC) which replaces the BS. A mobile terminal (MT) has a high probability to achieve high received SINR even near the cell edge by accessing nearby antennas.

In [6], the downlink channel capacity distribution of DAN-MIMO spatial multiplexing with single frequency reuse was investigated. However, the impact of the frequency reuse factor to the channel capacity was not discussed. In addition, a frequency-nonselective fading channel was assumed in [6]. In broadband wireless communications, the channel becomes frequency-selective due to the presence of many propagation paths with different time delays.

Block transmissions with CP insertion, such as orthogonal frequency division multiplexing (OFDM) transmission [7] and single-carrier transmission using frequency-domain equalization (SC-FDE) [8], are known as promising broadband data transmission techniques. In this paper, we consider a block transmission with CP insertion and derive a downlink spectral efficiency expression of broadband DAN-MIMO spatial multiplexing and the optimal power allocation (PA) which maximizes the spectral efficiency. The optimal PA requires perfect knowledge of the PA in the neighboring cells and needs to use an iterative method. Therefore, we propose 2 suboptimal PA schemes which do not need iteration; the first one requires partial knowledge of the PA in the neighboring cells and the second one requires no knowledge of PA at all. We evaluate the spectral efficiency distribution by Monte Carlo numerical computation method and discuss the impact of the frequency reuse factor on the spectral efficiency. It is shown that DAN allows the single frequency reuse and achieves higher spectral efficiency than CN. It is also shown that one of the proposed suboptimal PA scheme achieves almost the same spectral efficiency as the optimal PA scheme.

The remainder of this paper is organized as follows. In Section II, we show the downlink transmission models of DAN and CN. In Section III, we theoretically derive an expression for downlink spectral efficiency of broadband DAN-MIMO spatial multiplexing for a block transmission with CP insertion and give the optimal and suboptimal PA schemes. In Section IV, we evaluate the spectral efficiency distribution by Monte Carlo numerical computation method. Section V offers some conclusions.

978-1-4673-1881-5/12/$31.00 ©2012 IEEE

II. TRANSMISSION MODEL

A. Network model

Fig. 1 illustrates an example of a CCI model with the frequency reuse factor F=3. The center cell (i=0) is assumed to be the cell of interest. There are 6 CCI cells in the first tier and 12 CCI cells in the second tier (i=1~18).

Fig. 2 illustrates the hexagonal cell layout. DAN is assumed to have 7 distributed antennas while CN has 7 antennas co-located at each BS. A single MT having N_r receive antennas is assumed to exist in each cell. In DAN, distributed antennas are equidistantly distributed along a circle of radius $2R/3$, where R represents the cell radius. On the other hand, in CN, 7 antennas are co-located at the center of cell. Both in DAN and CN, N_t (≤ 7) transmit antennas are selected from 7 antennas for the downlink MIMO transmission. The antenna selection method is discussed in Section II-*B*.

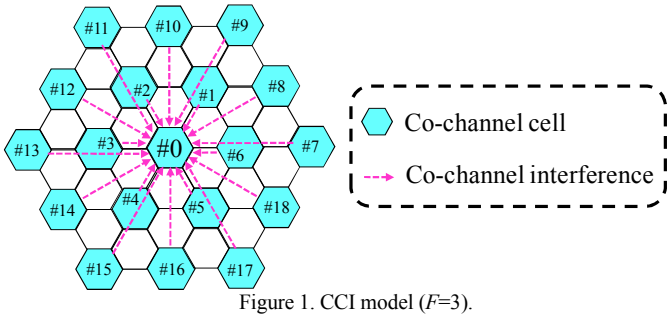

Figure 1. CCI model (F=3).

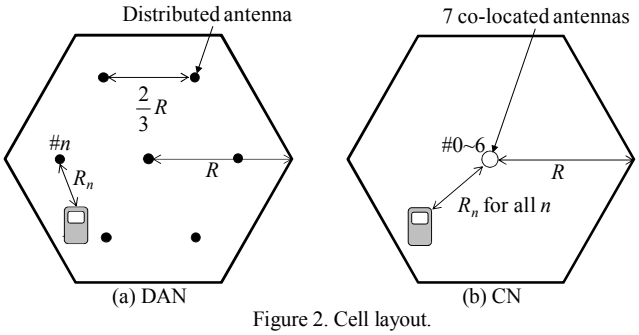

Figure 2. Cell layout.

B. Channel model

The broadband channel is characterized by distance-dependent path loss, log-normally distributed shadowing loss and frequency-selective fading. The average signal power $P_{r,n}$ received at MT for the signal transmitted from the nth (n=0~6) transmit antenna can be modeled as [2]

$$P_{r,n} = P_{t,n} \cdot R_n^{-\alpha} \cdot 10^{-\frac{\eta_n}{10}}, \tag{1}$$

where $P_{t,n}$ is the transmit power from the nth transmit antenna, R_n is the distance between the nth transmit antenna and MT, α is the path loss exponent, and η_n is the shadowing loss in dB having zero-mean and standard deviation σ_S. By introducing the normalized distance r_n=R_n/R and the normalized transmit power $p_{t,n} = P_{t,n} \cdot R^{-\alpha}$, Eq. (1) can be rewritten as

$$P_{r,n} = p_{t,n} \cdot \Omega_n, \tag{2}$$

where $\Omega_n = r_n^{-\alpha} \cdot 10^{-\eta_n/10}$.

Assuming a frequency-selective channel composed of L distinct paths, the channel impulse response $h_{m,n}(\tau)$ between the nth transmit antenna and the mth MT antenna is expressed as

$$h_{m,n}(\tau) = \sqrt{\Omega_n} \sum_{l=0}^{L-1} h_{m,n}^{(l)} \delta(\tau - \tau_{m,n}^{(l)}), \tag{3}$$

where $h_{m,n}^{(l)}$ and $\tau_{m,n}^{(l)}$ are respectively the complex-valued path gain and the time delay of the lth path with $E[\sum_{l=0}^{L-1} |h_{m,n}^{(l)}|^2] = 1$. In this paper, we assume a symbol-spaced time delay (i.e., $\tau_{m,n}^{(l)} = l$). $\delta(\tau)$ is the delta function.

Antenna selection is an important issue. In this paper, the transmit antennas are selected based on the instantaneous received signal power, i.e., N_t antennas having the largest sum $\Omega_n \sum_{m=0}^{N_r-1} \sum_{l=0}^{L-1} |h_{m,n}^{(l)}|^2$ of the squared path gains are selected for the downlink MIMO transmission.

III. SPECTRAL EFFICIENCY OF MIMO SPATIAL MULTIPLEXING IN A FREQUENCY-SELECTIVE CHANNEL

A. Spectral efficiency expression

In this paper, we assume a block transmission with CP insertion such as OFDM and SC-FDE. CP is much longer than the maximum time delay. N_t signal blocks, of N_c symbols each, are transmitted simultaneously from N_t selected transmit antennas.

After CP removal, the frequency-domain signal $Y_m(k)$ received on the mth MT antenna, m=0~N_r–1, in the cell of interest is expressed as

$$Y_m(k) = \sqrt{\frac{2E_s}{T_s}} \sum_{n=0}^{N_t-1} H_{m,n}(k) X_n(k) + Q_m(k) + Z_m(k) \tag{4}$$

for k=0~N_c–1, where $E_s = p_t \cdot T_s$ is the normalized total transmit symbol energy with $p_t = \sum_{n=0}^{N_t-1} p_{t,n}$ being the normalized total transmit power and T_s being the symbol length. The transfer function of the channel between the nth transmit antenna and the mth receive antenna in the cell of interest is denoted by $\{H_{m,n}(k);\ k=0\sim N_c-1\}$, where $H_{m,n}(k)$ is given as

$$H_{m,n}(k) = \sqrt{\Omega_n} \sum_{l=0}^{L-1} h_{m,n}^{(l)} \exp(-j2\pi k \tau_{m,n}^{(l)} / N_c). \tag{5}$$

$\{X_n(k);\ k=0\sim N_c-1\}$ is the frequency-domain signal representation for the block transmitted from the nth transmit antenna in the cell of interest. $\{Q_m(k);\ k=0\sim N_c-1\}$ is the frequency-domain CCI from the neighboring cells, expressed as

$$Q_m(k) = \sqrt{\frac{2E_s}{T_s}} \sum_{i \neq 0} \sum_{n=0}^{N_t-1} H_{m,n}^{(i)}(k) X_n^{(i)}(k), \tag{6}$$

where $\{H_{m,n}^{(i)}(k);\ k=0\sim N_c-1\}$ is the transfer function of the channel between the mth receive antenna in the cell of interest and the nth transmit antenna in the ith cell. $\{X_n^{(i)}(k);\ k=0\sim N_c-1\}$ is the frequency-domain signal representation for the block transmitted from the nth transmit antenna in the ith cell. $\{Z_m(k);\ k=0\sim N_c-1\}$ is the frequency-domain noise,

characterized by independent zero-mean complex-valued random variable having variance $2N_0/T_s$ with N_0 being the one-sided power spectrum density of additive white Gaussian noise (AWGN).

Since $Q_m(k)$ is the sum of the independent CCI from many transmit antennas in the neighboring cells, the CCI plus noise can be approximated as a complex-valued Gaussian variable $G_m(k) \equiv Q_m(k) + Z_m(k)$, according to the central limit theorem [2]. The variance $2\sigma^2(k)$ of $G_m(k)$ is expressed as

$$2\sigma^2(k) = \frac{2E_s}{T_s} \sum_{i \neq 0} \sum_{n=0}^{N_t-1} \Omega_n^{(i)} \Phi_n^{(i)}(k) + \frac{2N_0}{T_s}, \tag{7}$$

where $\Omega_n^{(i)} = \left(r_n^{(i)}\right)^{-\alpha} \cdot 10^{-\eta_n^{(i)}/10}$, and $r_n^{(i)}$ and $\eta_n^{(i)}$ are, respectively, the normalized distance and shadowing loss in dB between the MT in the cell of interest and the nth transmit antenna in the ith cell. $\Phi_n^{(i)}(k) = E[\left|X_n^{(i)}(k)\right|^2]$ is the transmit power of the nth transmit antenna in the ith cell; the optimal transmit power to maximize the spectral efficiency is derived in Section III-*B*. The total transmit power in each cell is assumed to be constant for all cells (i.e., $\sum_{k=0}^{N_c-1} \sum_{n=0}^{N_t-1} \Phi_n^{(i)}(k) = N_c$ for all i).

The signals received on N_r receive antennas can be expressed in the matrix form as

$$\begin{aligned} \mathbf{Y}(k) &= [Y_0(k), \cdots, Y_{N_r-1}(k)]^T \\ &= \sqrt{\frac{2E_s}{T_s}} \begin{bmatrix} H_{0,0}(k) & \cdots & H_{0,N_t-1}(k) \\ \vdots & \ddots & \vdots \\ H_{N_r-1,0}(k) & \cdots & H_{N_r-1,N_t-1}(k) \end{bmatrix} \begin{bmatrix} X_0(k) \\ \vdots \\ X_{N_t-1}(k) \end{bmatrix} + \begin{bmatrix} G_0(k) \\ \vdots \\ G_{N_r-1}(k) \end{bmatrix} \\ &= \sqrt{\frac{2E_s}{T_s}} \mathbf{H}(k)\mathbf{X}(k) + \mathbf{G}(k). \end{aligned} \tag{8}$$

In this paper, we define the spectral efficiency C (bps/Hz/cell) as the channel capacity per cell. Following [9], C is given as

$$C = \frac{1}{F} \cdot \frac{1}{N_c} \times \max_{\sum_{k=0}^{N_c-1} \mathrm{tr}[\mathbf{\Phi}(k)] = N_c} \sum_{k=0}^{N_c-1} \log_2 \det\left(\mathbf{I}_{N_r} + \Gamma(k)\mathbf{H}(k)\mathbf{\Phi}(k)\mathbf{H}^H(k)\right), \tag{9}$$

where the coefficient $1/F$ in Eq. (9) comes from the fact that the given system bandwidth W is divided into F sub-bands, each consisting of N_c/F subcarriers, and one sub-band is allocated to each cell. tr[.], det(.), and $(.)^H$ denote the trace operation, the determinant, and the Hermitian transpose operation, respectively. $\mathbf{I}_{N_r}$ is the $N_r \times N_r$ identity matrix. $\Gamma(k)$ is given as

$$\Gamma(k) = \frac{2E_s/T_s}{2\sigma^2(k)} = \frac{1}{\sum_{i \neq 0} \sum_{n=0}^{N_t-1} \Omega_n^{(i)} \Phi_n^{(i)}(k) + (E_s/N_0)^{-1}}. \tag{10}$$

$\mathbf{\Phi}(k) = E[\mathbf{X}(k)\mathbf{X}^H(k)]$ is the autocorrelation matrix of the transmit signal. The optimal $\mathbf{\Phi}(k)$, which maximizes Eq. (9), depends on whether the transmitter has channel state information (CSI) or not. In Section III-*B*, we will derive the optimal PA scheme which maximizes the spectral efficiency.

B. Optimal PA scheme

Since $\det(\mathbf{I}_{N_r} + \mathbf{AB}) = \det(\mathbf{I}_{N_t} + \mathbf{BA})$, where $\mathbf{A}$ and $\mathbf{B}$ are respectively $N_r \times N_t$ and $N_t \times N_r$ matrices, Eq. (9) can be rewritten as

$$C = \frac{1}{F} \cdot \frac{1}{N_c} \max_{\sum_{k=0}^{N_c-1} \mathrm{tr}[\mathbf{\Phi}(k)] = N_c} \sum_{k=0}^{N_c-1} \log_2 \det\left(\mathbf{I}_{N_t} + \Gamma(k)\mathbf{\Phi}(k)\mathbf{H}^H(k)\mathbf{H}(k)\right). \tag{11}$$

$\mathbf{H}^H(k)\mathbf{H}(k)$ is a square matrix and can be transformed by the eigenvalue decomposition as

$$\mathbf{H}^H(k)\mathbf{H}(k) = \mathbf{U}(k)\mathbf{\Lambda}(k)\mathbf{U}^H(k), \tag{12}$$

where $\mathbf{U}(k)$ is an $N_t \times N_t$ unitary matrix and $\mathbf{\Lambda}(k)$ is an $N_t \times N_t$ diagonal matrix having eigenvalues as its diagonal elements. From Eq. (12), Eq. (11) can be rewritten as

$$C = \frac{1}{F} \cdot \frac{1}{N_c} \times \max_{\sum_{k=0}^{N_c-1} \mathrm{tr}[\mathbf{\Phi}(k)] = N_c} \sum_{k=0}^{N_c-1} \log_2 \det\begin{pmatrix} \mathbf{I}_{N_t} \\ +\Gamma(k)\mathbf{U}^H(k)\mathbf{\Phi}(k)\mathbf{U}(k)\mathbf{\Lambda}(k) \end{pmatrix}. \tag{13}$$

1) Known CSI case

When perfect knowledge of $\Gamma(k)$ and $\mathbf{H}(k)$ is available at the transmitter, the optimal $\mathbf{\Phi}(k)$ which maximizes the determinant can be found. From Hadamard's inequality [10], the determinant is maximized when the matrix $\mathbf{I}_{N_t} + \Gamma(k)\mathbf{U}^H(k)\mathbf{\Phi}(k)\mathbf{U}(k)\mathbf{\Lambda}(k)$ is diagonal. Thus, the optimal $\mathbf{\Phi}(k)$ is given as

$$\mathbf{\Phi}(k) = \mathbf{U}(k)\tilde{\mathbf{\Phi}}(k)\mathbf{U}^H(k), \tag{14}$$

where $\tilde{\mathbf{\Phi}}(k)$ is an $N_t \times N_t$ positive semidefinite diagonal matrix. From Eq. (14), Eq. (13) can be rewritten as

$$\begin{aligned} C &= \frac{1}{F} \cdot \frac{1}{N_c} \max_{\sum_{k=0}^{N_c-1} \mathrm{tr}[\tilde{\mathbf{\Phi}}(k)] = N_c} \sum_{k=0}^{N_c-1} \log_2 \det\left(\mathbf{I}_{N_t} + \Gamma(k)\tilde{\mathbf{\Phi}}(k)\mathbf{\Lambda}(k)\right) \\ &= \frac{1}{F} \cdot \frac{1}{N_c} \max_{\sum_{k=0}^{N_c-1} \sum_{n=0}^{N_t-1} \tilde{\Phi}_n(k) = N_c} \sum_{k=0}^{N_c-1} \sum_{n=0}^{N_t-1} \log_2\left(1 + \Gamma(k)\tilde{\Phi}_n(k)\Lambda_n(k)\right) \end{aligned}, \tag{15}$$

where $\Lambda_n(k)$ and $\tilde{\Phi}_n(k)$ are the nth eigenvalue and the transmit power allocated to the nth eigenmode of the kth frequency, respectively.

The maximization problem of Eq. (15) can be converted into a concave optimization problem under the total transmit power constraint [11] for the given $\Gamma(k)$. Following [11], the optimal solution is given as (for the sake of brevity, the derivation is omitted)

$$\tilde{\Phi}_n(k) = \max\left\{\frac{1}{\mu} - \frac{1}{\Gamma(k)\Lambda_n(k)}, 0\right\} \tag{16}$$

for n=0~N_t–1 and k=0~N_c–1, where μ is chosen to satisfy $\sum_{k=0}^{N_c-1} \sum_{n=0}^{N_t-1} \tilde{\Phi}_n(k) = N_c$. It can be seen from Eq. (16) that the optimal PA is done based on the water-filling theory across eigenmodes and frequencies. The spectral efficiency is given as

$$C_{CSI} = \frac{1}{F} \cdot \frac{1}{N_c} \sum_{k=0}^{N_c-1} \sum_{n=0}^{N_t-1} \max\left\{ \log_2\left(\frac{1}{\mu} \Gamma(k) \Lambda_n(k) \right), 0 \right\}. \quad (17)$$

In fact, $\Gamma(k)$ and $\widetilde{\mathbf{\Phi}}(k)$ interact with each other because the PA given as Eq. (16) is done in the neighboring CCI cells also. Therefore, Eq. (17) is not a closed form. In this paper, the optimal $\Gamma(k)$ and $\widetilde{\mathbf{\Phi}}(k)$ are numerically found by using an iterative method as follows.

Step 1. Calculate $\widetilde{\mathbf{\Phi}}(k)$ in the cell of interest by setting $\Phi_n^{(i)}(k) = 0$ for i=1~18 and n=0~N_t–1.

Step 2. Calculate $\Gamma(k)$ and $\widetilde{\mathbf{\Phi}}(k)$ in the neighboring cells by using $\widetilde{\mathbf{\Phi}}(k)$ in the cell of interest.

Step 3. Calculate $\Gamma(k)$ and $\widetilde{\mathbf{\Phi}}(k)$ in the cell of interest by using $\widetilde{\mathbf{\Phi}}(k)$ in the neighboring cells.

Step 4. Repeat the steps 2 and 3 until the normalized difference in $\Gamma(k)$ from the previous iteration is smaller than 0.01 for all k.

The spectral efficiency is obtained by substituting the optimal $\Gamma(k)$ and $\widetilde{\mathbf{\Phi}}(k)$ into Eq. (15).

2) Unknown CSI case

When $\Gamma(k)$ and $\mathbf{H}(k)$ are not available at the transmitter, equal PA (i.e., $\widetilde{\mathbf{\Phi}}_n(k) = (1/N_t)\mathbf{I}_{N_t}$, k=0~N_c–1) maximizes the spectral efficiency [9]. In this case, Eq. (10) is rewritten as

$$\Gamma(k) = \Gamma = \frac{1}{\sum_{i \neq 0} \sum_{n=0}^{N_t-1} \Omega_n^{(i)} / N_t + (E_s / N_0)^{-1}} \quad (18)$$

and the spectral efficiency is given as

$$C_{noCSI} = \frac{1}{N_c} \sum_{k=0}^{N_c-1} \sum_{n=0}^{N_t-1} \log_2\left(1 + \frac{1}{N_t} \Gamma \cdot \Lambda_n(k) \right). \quad (19)$$

The transmission scheme which achieves the spectral efficiency of Eq. (17) is called the eigenbeam-space division multiplexing (E-SDM) and the transmission scheme which achieves the spectral efficiency of Eq. (19) is called SDM. E-SDM achieves higher spectral efficiency than SDM [9].

C. Suboptimal PA schemes

Although water-filling PA (E-SDM) given as Eq. (17) outperforms equal PA (SDM), it requires the knowledge of $\widetilde{\mathbf{\Phi}}(k)$ in the neighboring cells and needs to use the iterative method. Therefore, we propose 2 suboptimal PA schemes which do not need to use the iterative method.

1) Known partial information about CCI

When the transmitter knows which antennas are used in the neighboring cells, the approximated $\Gamma(k)$, $\hat{\Gamma}$ can be obtained by assuming that equal PA is done in the neighboring cells as

$$\hat{\Gamma} = \frac{1}{\sum_{i \neq 0} \sum_{n=0}^{N_t-1} \Omega_n^{(i)} / N_t + (E_s / N_0)^{-1}}. \quad (20)$$

Therefore, the suboptimal PA (in this paper, referred to as "suboptimal PA-1") is given as

$$\widetilde{\Phi}_n(k) = \max\left\{ \frac{1}{\mu} - \frac{1}{\hat{\Gamma} \cdot \Lambda_n(k)}, 0 \right\}. \quad (21)$$

2) Unknown information about CCI

When the transmitter does not have knowledge of the neighboring cells, another approximated $\Gamma(k)$, $\hat{\Gamma}'$ can be obtained by assuming that there is no CCI from the neighboring cells (i.e., $\hat{\Gamma}' = E_s/N_0$). Therefore, the suboptimal PA (in this paper, referred to as "suboptimal PA-2") is given as

$$\widetilde{\Phi}_n(k) = \max\left\{ \frac{1}{\mu} - \frac{1}{\hat{\Gamma}' \cdot \Lambda_n(k)}, 0 \right\}. \quad (22)$$

It can be seen from Eq. (21) and Eq. (22) that these suboptimal PA schemes operate independently in each cell. Therefore, there is no need to use the iterative method.

IV. Numerical Evaluation

As the frequency reuse factor F increases, the CCI can be reduced; however the bandwidth W/F allocated to each cell decreases (i.e., the spectral efficiency C decreases). Therefore, the optimal F which maximizes the spectral efficiency C is discussed below. Assuming the hexagonal cell layout shown in Fig. 2, the distribution of spectral efficiency is evaluated by Monte Carlo numerical computation method using Eqs. (17) and (19) for the comparison between DAN and CN.

A. Numerical evaluation condition

The cumulative distribution function (CDF) of the spectral efficiency is measured by randomly changing the MT location in each cell. From the CDF curves, the 10%-outage capacity, below which the spectral efficiency falls at a probability of 10%, is obtained. The numerical evaluation condition is summarized in Table I. We assume a frequency-selective block Rayleigh fading channel having a symbol-spaced L=16-path uniform power delay profile (i.e., $E[|h_{m,n}^{(l)}|^2] = (1/L)$). Each pair of transmit and receive antennas is assumed to experience independent fading. Independent shadowing is assumed between distributed antennas.

TABLE I. NUMERICAL EVALUATION CONDITION.

System	Frequency reuse factor	F=1,3,4,7
	Block size	N_c=256
Channel	Path loss exponent	α=3.5
	Shadowing loss standard deviation	σ_S=7.0 (dB)
	Fading	Frequency-selective block Rayleigh (i.i.d.) with L=16-path uniform power delay profile

B. Outage capacity

Fig. 3 shows the downlink 10%-outage capacity of DAN-MIMO spatial multiplexing as a function of the frequency reuse factor F. The normalized total transmit E_s/N_0 is set to infinite (i.e., an interference limited environment). For comparison, the downlink 10%-outage capacity of CN-MIMO spatial multiplexing is also plotted. It can be seen from Fig. 3 that DAN achieves significantly higher 10%-outage capacity

than CN. This is because, in DAN, distributed antennas near the MT can be chosen and hence, the impact of path loss can be significantly suppressed.

It can also be seen from Fig. 3 that the 10%-outage capacity of DAN has a different trend from that of CN when F is changed. In CN, the 10%-outage capacity is maximized when F=3 or 4 because strong CCI exists when F=1. However, in DAN, the 10%-outage capacity can be maximized when F=1 except for the case of SDM (equal PA) with N_t=N_r=4. This is because, in DAN, the received SINR can be increased without increasing F. However, when SDM with N_t=N_r=4 is used in DAN, the same transmit power is allocated to the antennas located far from MT. As a consequence, the received SINR cannot be sufficiently increased and therefore, F has to be increased to reduce the CCI.

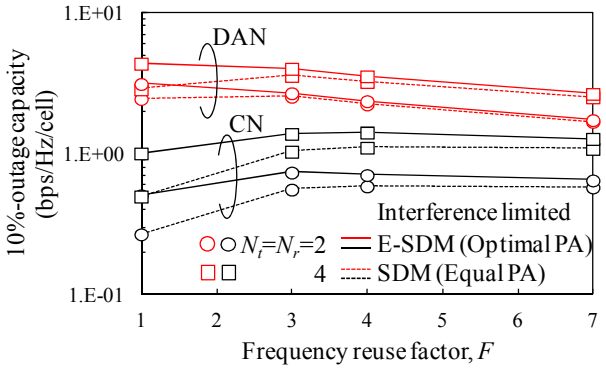

Figure 3. 10% outage capacity.

C. Comparison of PA schemes

It can be seen from Fig. 3 that E-SDM (optimal PA) achieves higher 10%-outage capacity than SDM (equal PA). However, the optimal PA scheme requires perfect knowledge of the PA information in the neighboring cells. Next, we compare the PA schemes. Fig. 4 shows the 10%-outage capacity of DAN-MIMO spatial multiplexing with the normalized total transmit E_s/N_0 as a parameter for various PA schemes when N_t=N_r=2. It can be seen from Fig. 4 that the suboptimal PA-1 scheme achieves almost the same 10%-outage capacity as the optimal PA scheme irrespective of the total transmit power. On the other hand, the 10%-outage capacity using the suboptimal PA-2 scheme degrades when the total transmit power is high. This is because the suboptimal PA-2 scheme does not account for CCI, although CCI increases as the total transmit power increases.

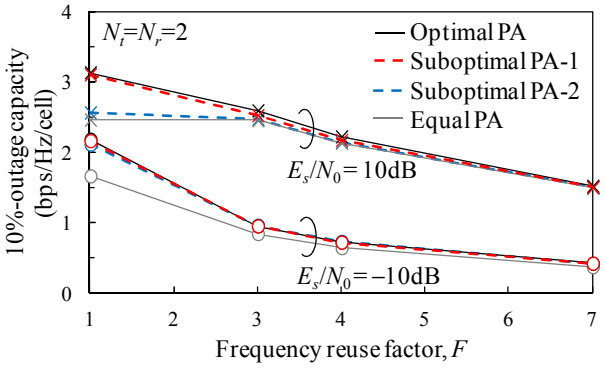

Figure 4. Comparison of PA schemes.

V. Conclusion

Assuming block transmission with CP insertion, we theoretically derived an expression for the downlink spectral efficiency of DAN-MIMO spatial multiplexing in a multi-cell environment. We then proposed the optimal and suboptimal PA schemes for DAN-MIMO spatial multiplexing. We evaluated the spectral efficiency distribution by Monte Carlo numerical computation method to show that DAN allows single frequency reuse and achieves higher spectral efficiency compared to CN. It was also shown that one of the suboptimal PA scheme achieves almost the same spectral efficiency as the optimal (water-filling) PA scheme.

References

[1] E. Biglieri, R. Calderbank, A. Constantinides, A. Goldsmith, A. Paulraj, and H. V. Poor, *MIMO Wireless Communications*, Cambridge University Press, 2007.

[2] A. Goldsmith, *Wireless Communication*, Cambridge University Press, 2005.

[3] A. A. M. Saleh, A. J. Rustako, and R. S. Roman, "Distributed antennas for indoor radio communications," IEEE Trans. Commun., vol. 35, no. 12, pp. 1245-1251, Dec. 1987.

[4] H. Hu, Y. Zhang, and Y. Yao, *Distributed antenna systems; open architecture for future wireless communications*, Auerbach Pub., 2007.

[5] E. Kudoh and F. Adachi, "Study of a multi-hop communication in a virtual cellular system," Proc. 6th International Symposium on Wireless Personal Multimedia Communications (WPMC), vol.3, pp.261-265, Yokosuka, Japan, 19-22 Oct. 2003.

[6] W. Feng, Y. Li, S. Zhou, J. Wang and M. Xia, "Downlink capacity of distributed antenna systems in a multi-cell environment," Proc. 2009 IEEE Wireless Communications and Networking Conference (WCNC2009) , pp. 1-5, Budapest, Hungary, 5-8 Apr. 2009.

[7] A. Czylwik, "Comparison between adaptive OFDM and single carrier moduration with frequency domain equalization," Proc. 47th IEEE Vehicular Technology Conference (VTC1997), vol. 2, pp. 865-869, Arizona, United States, 4-7 May 1997.

[8] D. Falconer, S. L. Ariyavisitakul, A. benyamin-Seeyar, and B. Eidson, "Frequency domain equalization for single-carrier broadband wireless systems," IEEE Commun. Mag., vol. 40, no. 4, pp. 58-66, Apr. 2002.

[9] A. Paulraj R. Nabar and D. Gore, *Introduction to Space-Time Wireless Communications*, Cambridge University Press, 2003.

[10] T. M. Cover and A. E. Gamal, "An information-theoretic proof of Hadamard's inequality," IEEE Trans. Inform. Theory, vol. 29, no. 6, pp. 930-931, Nov. 1983.

[11] S. Boyd and L. Vandenberghe, *Convex Optimization*, Cambridge, 2006.